J. Fluid Mech. (1971), *vol.* 48, *part* 2, *pp.* 365–384
Printed in Great Britain

Stability of time-dependent rotational Couette flow Part 2. Stability analysis

By C. F. CHEN

Department of Mechanical & Aerospace Engineering,
Rutgers University – The State University of New Jersey

AND R. P. KIRCHNER

Mechanical Engineering Department, Newark College of Engineering

(Received 1 September 1970)

The stability of the flow induced by an impulsively started inner cylinder in a Couette flow apparatus is investigated by using a linear stability analysis. Two approaches are taken; one is the treatment as an initial-value problem in which the time evolution of the initially distributed small random perturbations of given wavelength is monitored by numerically integrating the unsteady perturbation equations. The other is the quasi-steady approach, in which the stability of the instantaneous velocity profile of the basic flow is analyzed. With the quasi-steady approach, two stability criteria are investigated; one is the standard zero perturbation growth rate definition of stability, and the other is the momentary stability criterion in which the evolution of the basic flow velocity field is partially taken into account. In the initial-value problem approach, the predicted critical wavelengths agree remarkably well with those found experimentally. The kinetic energy of the perturbations decreases initially, reaches a minimum, then grows exponentially. By comparing with the experimental results, it may be concluded that when the perturbation kinetic energy has grown a thousand-fold, the secondary flow pattern is clearly visible. The time of intrinsic instability (the time at which perturbations first tend to grow) is about $\frac{1}{4}$ of the time required for a thousandfold increase, when the instability disks are clearly observable. With the quasi-steady approach, the critical times for marginal stability are comparable to those found using the initial-value problem approach. The predicted critical wavelengths, however, are about $1\frac{1}{2}$ to 2 times larger than those observed. Both of these points are in agreement with the findings of Mahler, Schechter & Wissler (1968) treating the stability of a fluid layer with time-dependent density gradients. The zero growth rate and the momentary stability criteria give approximately the same results.

1. Introduction

The results of an experimental investigation of the stability of time-dependent rotational Couette flow induced by an impulsively started inner cylinder have been presented by Kirchner & Chen (1970, hereafter referred to as I). The initial

laminar flow evolves into a secondary flow pattern which consists of a series of Taylor-type vortices spaced approximately evenly along the inner cylinder. The average spacing between the vortices and the critical time for the first appearance of the instabilities decrease as the rotational speed of the inner cylinder increases. In this paper, we present the results of a stability analysis of this flow phenomenon.

The stability analysis for the time-independent basic flows is conceptually straightforward. One introduces into the flow field perturbations of small amplitude but of different wavelengths. These perturbations may decay or grow depending on the properties of the basic flow, and the rate of growth or decay is a function of the wave-number. For a given flow, there are generally two particular waves which are neutrally stable thus delineating the stable and unstable regions; a marginal stability curve may be constructed. This method has been eminently successful in the stability analysis of the rotating Couette flows, laminar boundary-layer flows and the Bénard convection problem to name a few. In a basically time-dependent flow, this concept cannot be carried over since the perturbations are continuously interacting with the basic flow which is itself evolving in time.

If one is certain that the growth of the perturbations once started will be much faster than the evolution of the basic flow, then a quasi-steady approach can be taken. With this approach the instantaneous velocity profile is analyzed for stability in much the same way as for a steady-state problem. Since the history of the flow is ignored, one is never sure *a priori* of the applicability of this method. Shen (1961) has advanced the idea of momentary stability in which the time-dependent feature of the basic flow is taken into account. His idea is that an accelerating basic flow is classified as momentarily unstable only when the growth rate of the perturbations exceeds that of the basic flow. The attractiveness of the quasi-steady approach is that the linear perturbation equations reduce to an eigenvalue problem (even with the momentary stability criterion), whose solution yields both the critical wavelength and critical time without introducing arbitrary initial conditions. Morton (1957), Lick (1965) and Currie (1967) have used this approach in treating Bénard problems with time-dependent temperature profile. Conrad & Criminale (1965) have taken the quasi-steady approach in a non-linear formulation of the time-dependent basic flow problems. Using the variational technique of Serrin (1959), a set of linear equations was obtained. They have treated the problem of rotating Couette flow with sinusoidal modulation of the inner cylinder, which was investigated experimentally by Donnelly (1964), using the concept of momentary stability. Their results were conservative since only the sufficient condition for stability is determined.

Another way to approach the problem is to solve the linear stability equation as an initial-value problem. Perturbations of small magnitude and of given wavelengths are initially distributed in the flow field, and their progress in time is obtained by integration of the perturbation equations. The growth or decay of the perturbation kinetic energy would indicate whether the flow is unstable or stable. With the advent of high-speed computers, this method has become

increasingly popular. Meister (1963) has used this approach together with the Galerkin method to examine a time-dependent Couette flow with narrow gap. The steady Couette flow established in an annulus is disturbed by a sudden increase of rotational speed of the inner cylinder. His results show that as the rotational speed of the inner cylinder is increased beyond a certain critical value, the kinetic energy of the perturbations grows without limit. Later, Meister & Münzner (1966) have used the same approachs to treat problems of narrow-gap Couette flow with sinusoidal modulation. Their results agree with the experimental results of Donnelly (1964). More recently, Thompson (1968) has used numerical integration to study the stability of flow induced by an impulsively started cylinder in a large container to compare with experimental results of Chen & Christensen (1967). His results are discussed in § 2.3. Foster (1965, 1969) and Mahler, Schechter & Wissler (1968) have used this approach to examine the stability of fluid layers with time-dependent density gradients. By comparing the results of quasi-steady analysis to those of the initial-value problem approach, Mahler *et al.* found that the critical times for intrinsic instability (the time when the perturbations first tend to grow) predicted by these two methods are in reasonable agreement. The critical wave-number of that wave which tends to grow first, as predicted by the quasi-steady method, is about half of that predicted by the initial-value problem.

In this paper, starting with the linear stability equation, we have performed stability analysis both with the initial-value problem approach and the quasi-steady approach on the problem of an impulsively started inner cylinder in a Couette flow apparatus. These two methods of solution are presented in §§ 2 and 3, and a discussion of the results obtained is presented in § 4. We have found that the critical wavelength predicted by the initial-value problem agrees well with the experimental results of I, and that when the kinetic energy of the perturbations has grown a thousandfold, the secondary flow pattern is clearly observable. We have reached the same general conclusion about the comparison between the initial-value problem and the quasi-steady analysis as that reached by Mahler *et al.* The zero growth rate and the momentary stability criteria gave approximately the same results.

2. Initial-value problem

2.1. *Basic equations*

Consider two concentric cylinders of radii R_1 and R_2 with $R_1 < R_2$. Let the axis of the inner cylinder be along the z' axis of a cylindrical co-ordinate system (r', θ, z'). The outer cylinder is kept stationary; the inner cylinder is impulsively started at $t = 0$ and maintained at a constant surface speed V_0'. The time-dependent velocity field within the annulus is denoted by $V'(r', t)$. Assuming axisymmetric perturbations periodic in z' in the velocity components and in the pressure,

$$u'(r', t)\cos\alpha z', \quad v'(r', t)\cos\alpha z',$$

$$w'(r', t)\sin\alpha z', \quad p'(r', t)\cos\alpha z',$$

the linearized equations of motion become

$$\left[D'D'^*-\alpha^2-\frac{1}{\nu}\frac{\partial}{\partial t}\right](D'D'^*-\alpha^2)\,u' = \frac{2V'v'\alpha^2}{\nu r'}, \tag{1}$$

$$\left[D'D'^*-\alpha^2-\frac{1}{\nu}\frac{\partial}{\partial t}\right]v' = \frac{u'D'^*V'}{\nu}, \tag{2}$$

when w' and p' are eliminated. In the above equations

$$D' = \partial/\partial r', \quad D'^* = D' + 1/r',$$

and ν is the kinematic viscosity. The boundary conditions, after using the continuity equation are

$$u' = v' = D'^*u' = 0, \quad \text{at} \quad r' = R_1 \quad \text{and} \quad R_2. \tag{3}$$

With R_1 as the reference length, V_0' the reference velocity, (1) and (2) assume the following non-dimensional form

$$[DD^*-\kappa^2-\partial/\partial\tau](DD^*-\kappa^2)\,u = 2Re\,\kappa^2 Vv/r, \tag{4}$$

$$[DD^*-\kappa^2-\partial/\partial\tau]\,v = Re\,uD^*V, \tag{5}$$

in which the non-dimensional variables are now unprimed. The non-dimensional time and wave-number are defined as

$$\tau = \nu t/R_1^2, \quad \kappa = \alpha R_1,$$

and the Reynolds number is $Re = R_1V_0'/\nu$. The boundary conditions become

$$u = v = D^*u = 0 \quad \text{at} \quad r = 1 \quad \text{and} \quad R(\equiv R_2/R_1). \tag{6}$$

The basic velocity field is governed by

$$\partial V/\partial\tau = DD^*V, \tag{7}$$

with the initial and boundary conditions

$$V(1,0) = 1; \quad V(r,0) = 0 \quad \text{for} \quad 1 < r \leqslant R, \tag{8a}$$

$$V(1,\tau) = 1, \quad V(R,\tau) = 0, \tag{8b}$$

which may be solved by transform methods as is shown in § 3. However, since (4) and (5) will be solved by numerical means, we shall integrate (7) numerically also.

Following Thompson (1968), we introduce ψ which is defined as

$$\psi = (DD^*-\kappa^2)\,u. \tag{9}$$

Equation (4) becomes

$$\partial\psi/\partial\tau = (DD^*-\kappa^2)\,\psi - 2Re\,\kappa^2 Vv/r, \tag{10}$$

and (5) is rearranged to become

$$\partial v/\partial\tau = (DD^*-\kappa^2)\,v - Re\,uD^*V. \tag{11}$$

Equations (7), (10) and (11) prescribe the time evaluation of V, ψ and v and (9) defines ψ in terms of u. The velocity components satisfy boundary conditions (6) and (8). The boundary conditions on ψ may be obtained from (9),

$$\psi = \left(\frac{\partial^2}{\partial r^2}+\frac{1}{r}\frac{\partial}{\partial r}-\frac{1}{r^2}-\kappa^2\right)u = \frac{\partial^2 u}{\partial r^2} \quad \text{at} \quad r = 1 \quad \text{and} \quad R. \tag{12}$$

The perturbation kinetic energy per wavelength E_p and the basic flow kinetic energy per wavelength E_b are defined as follows:

$$\left.\begin{aligned} E_p &= \pi \int_1^R r\left[u^2+v^2+\frac{1}{\kappa^2}(D^*u)^2\right]dr, \\ E_b &= 2\pi \int_1^R rV^2\,dr, \end{aligned}\right\} \tag{13}$$

in which a normalizing constant $(\pi\rho V_0'^2 R_1^2)/\kappa$ is deleted.

2.2. *Computation procedure and difference equations*

The procedure of calculation is to first assume small random values of ψ at all interior grid points since the boundary values of ψ depends on the second derivative of u, which is not known *a priori*. Then (9) is solved for u; the boundary values of ψ can now be evaluated using (12). V, ψ, and v are then advanced in time according to (7), (10) and (11). For V and v, the values at interior grid points as well as those on the boundary are known. However, ψ is only known at all interior points. The procedure may now be repeated to obtain values at the next time step.

Let the annular region $1 \leqslant r \leqslant R$ be divided into J equal intervals, with $j = 0$ and J at the boundary points. The subroutine RANDU of the IBM system/360 Scientific Subroutine Package is used to generate random distribution of ψ. Random numbers are generated between 0 and 1, and these are multiplied by 10^{-4} so that the initial disturbances are small. The ψ-equation (9) is solved by the method of successive over-relaxation (Todd 1962). The $(k+1)$th iterate of u at grid point j and the nth time step is

$$u^n_{j,k+1} = \frac{\omega}{\lambda_j}[\alpha_j u^n_{j+1,k} + \beta_j u^n_{j-1,k+1} - (\Delta r)^2 \psi^n_j] - (\omega-1)\,u^n_{j,k} \quad (j = 1, 2, \ldots, J-1). \tag{14}$$

where

$$\begin{aligned} \alpha_j &= 1+(\Delta r)/2r_j, \\ \beta_j &= 1-(\Delta r)/2r_j, \\ \lambda_j &= 2+(\Delta r)^2(\kappa^2+r_j^{-2}), \end{aligned}$$

and ω is the relaxation factor. Iterations are terminated when the maximum relative error of two successive iterates is within 10^{-3}. For the very first calculation, the initial values of u are put at zero; for any subsequent time step, the initial values of u are those of the previous time step. The number of iterations needed is then reduced by a substantial amount. The optimum relaxation factor ω for a given grid size is a function of the wave-number κ. For the range of wave-numbers encountered, the optimum relaxation factors have been determined by numerical experimentation; these range from 1·96 for $\kappa = 0{\cdot}6$ linearly decreasing to 1·7 at $\kappa = 8{\cdot}5$. The number of iterations needed for random distributions of ψ and initial value of $u = 0$ ranges from 29 for $\kappa = 8$ and 113 for $\kappa = 1{\cdot}5$ for $\Delta r = 2{\cdot}5 \times 10^{-2}$.

For the parabolic equation, we have chosen the explicit scheme of integration. Although an implicit scheme may be less time-consuming because of its inherent numerical stability, the necessity of using an iteration procedure to

obtain the boundary values of ψ makes such time saving doubtful. The explicit difference equations for V, ψ, and v are quite similar; the equations are presented in terms of a general variable Q. At the grid point j, the value of Q at the $(n+1)$th time step is (Richtmeyer & Morton 1967)

$$Q_j^{n+1} = \frac{\Delta\tau}{(\Delta r)^2}\left\{\alpha_j Q_{j+1}^n + \beta_j Q_{j-1}^n + \left[\frac{(\Delta r)^2}{\Delta\tau} - \lambda_j\right] Q_j^n + F_j(Q)\right\}, \tag{15}$$

where

$$F_j(Q)\begin{cases} = \kappa^2(\Delta r)^2 V_j^n, & \text{for} \quad Q = V, \\ = 2Re\,\kappa^2 V_j^n v_j^n (\Delta r)^2/r_j, & \text{for} \quad Q = \psi, \\ = -\frac{1}{2}Re\,(\Delta r)\, u_j^n[V_{j+1}^n - V_{j-1}^n + 2(\Delta r)\, V_j^n/r_j], & \text{for} \quad Q = v, \end{cases}$$

in which $\Delta\tau/(\Delta r)^2 < 0{\cdot}5$ to ensure numerical stability. The boundary conditions for the velocity components are

$$\left.\begin{aligned} V_0 = 1, \quad V_J = 0, \\ u_0 = v_0 = u_J = v_J = 0, \end{aligned}\right\} \quad \text{for all } n. \tag{16}$$

To obtain the boundary conditions on ψ, we use the fact that the first derivative of u is zero at the boundary, and u would be symmetric if extended beyond the boundary (Thompson 1968).

$$\left.\begin{aligned} \psi_0^n &= \frac{1}{(\Delta r)^2}[u_1^n + u_{-1}^n - 2u_0^n] = \frac{2u_1^n}{(\Delta r)^2}, \\ \psi_J^n &= \frac{2u_{J-1}}{(\Delta r)^2}. \end{aligned}\right\} \tag{17}$$

The kinetic energy terms E_p and E_b (13) are obtained by using Simpson's rule.

2.3. *Results and discussion*

All calculations were made for a radius ratio η $(= 1/R)$ of 0·2. Although the data given in I were obtained for a radius ratio of 0·1, more recent data of Liu (1971) for a radius ratio of 0·2 showed no discernible difference in the critical time when the instabilities become observable. This is because even at a radius ratio of 0·2, at the time of observable instabilities, the outer cylinder has had no appreciable influence on the basic flow velocity distribution. The reduction in computation time by halving the gap width is of course considerable. Perturbations are introduced at $\tau = 0$ when the cylinder is impulsively started. Foster (1965) has shown that for the time-dependent Bénard problem if the perturbations are introduced at a later time, the growth curve of the perturbation kinetic energy is correspondingly shifted to a later time. We feel that in a physical experiment, disturbances are most likely to occur at the time when the inner cylinder is impulsively started. Mahler *et al.* (1968) also introduced the perturbations initially when treating the time-dependent Bénard problem. In the presentation of results, the perturbation kinetic energy is normalized with respect to its initial value and is denoted by $E = E_p/E_{p,\tau=0}$.

The number of grid points to be used in the annulus $1 \leqslant r \leqslant 5$ should give accurate results with the least amount of computation time. The two-fold

objectives are met with $J = 160$ or $\Delta r = 0{\cdot}025$. This is illustrated in figure 1 in which the growth curves of the perturbation kinetic energy at $Re = 400$ are shown for $J = 40, 80, 160$ and 320. It is noted that since $\Delta\tau \sim (\Delta r)^2$, the computational times increase approximately fourfold for each successive J value used.

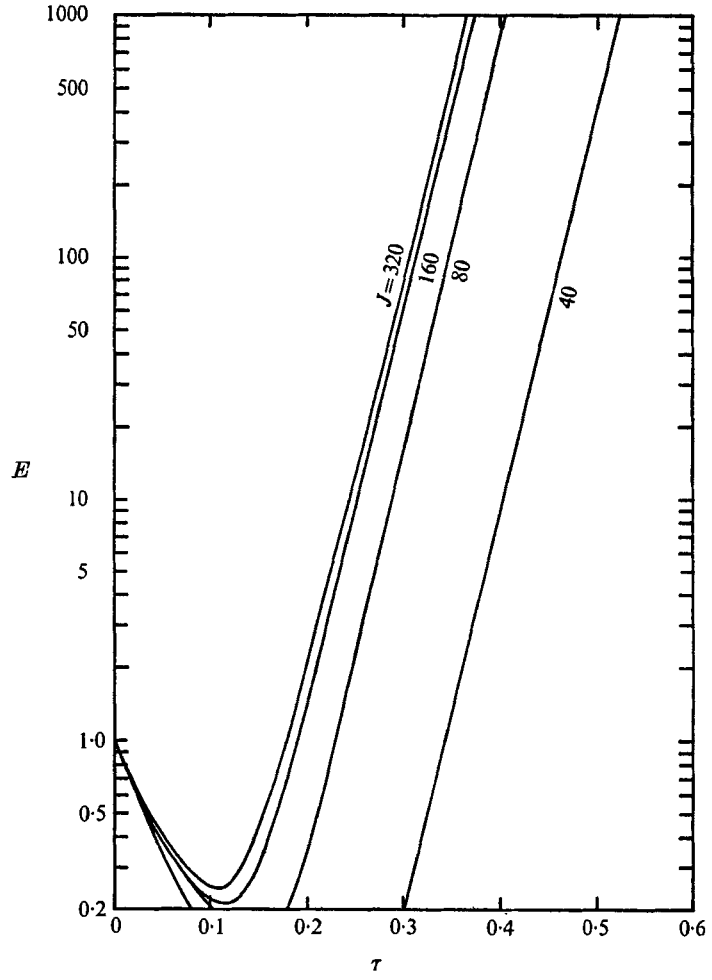

FIGURE 1. Effect of number of grid points $(J+1)$ on the accuracy of results for $Re = 400$.

The relative difference in times at the minima of the curves for $J = 160$ and $J = 230$ is approximately 5 % and the relative errors decrease at times when the perturbation energy has attained ten- a hundred- and a thousand-fold growth. In cases of lower Reynolds numbers, since the time involved is longer, the relative error decreases accordingly. With $J = 160$, the results obtained for different initial sets of random numbers have a relative error of less than 5 % for all the above mentioned critical times.

Calculations have been made for $Re = 50, 100, 150, 200, 300$ and 400. The value of $\Delta\tau/(\Delta r)^2$ was chosen to be 0·2 for $Re \geqslant 150$ and 0·4 for $Re = 50$ and 100. The smaller value was chosen for the larger values of Re so that the number of

iterations needed for each successive time step is not excessive. For each of the Reynolds numbers chosen, the growth of the perturbation kinetic energy is calculated for different values of the wave-number κ; that particular value of κ which gives the fastest growing perturbation is the critical wave-number. For all cases calculated, the growth rate of the perturbation kinetic energy presents a very shallow maximum with respect to the wave-number as shown in figure 2 for $Re = 400$. The perturbation kinetic energy at $\tau = 0{\cdot}02$ is shown as a function

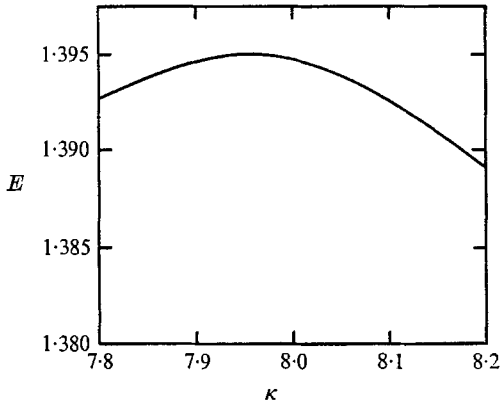

FIGURE 2. Determination of the fastest-growing wave, $Re = 400$, $\tau = 0{\cdot}02$.

			Critical times to reach				
Re	κ_{crit}	Z/R_1	E_m	E_{rm}	E_1	E_2	E_3
50	1·45	4·333	0·2215	0·2580	0·764	1·051	1·344
100	2·85	2·205	0·0810	0·0890	0·213	0·277	0·340
150	4·02	1·562	0·0447	0·0482	0·108	0·139	0·168
200	5·10	1·232	0·0292	0·0312	0·0690	0·0870	0·105
300	6·75	0·930	0·0165	0·0177	0·0380	0·0473	0·0566
400	7·96	0·789	0·0115	0·0120	0·0254	0·0313	0·0372

TABLE 1. Summary of results of the initial-value problem

of κ, and the critical value is 7·96. It has been our experience that after the perturbation kinetic energy has increased beyond its original value, i.e. $E > 1$, the growth rates of the different waves stay sensibly constant. This means whichever wave attains the highest rate of growth beyond $E = 1$, it will remain the fastest growing wave. The critical wave-numbers for all cases considered together with the non-dimensional wavelength $Z/R_1 = 2\pi/\kappa_{crit}$ are summarized in table 1. The non-dimensional wavelength as calculated is compared with those reported in I by Liu (1971) in figure 3. The agreement is quite good.

The evolution of the kinetic energy of the perturbations at the critical wave-numbers for all the cases considered are shown in figure 4 together with the kinetic energy of the basic flow E_b. It should be noted that time scale for $Re = 50$ and for E_b is compressed five-fold. Due to viscous damping, the perturbation

kinetic energy decreased intially. As energy is being fed from the basic flow to the perturbation flow, the initial decay of the perturbation kinetic energy is arrested and it reaches a minimum then grows exponentially. The time at which the perturbation kinetic energy is at the minimum is termed the critical time of intrinsic instability. The higher the Reynolds number, the sooner the minimum kinetic energy point is reached and the larger the rate of growth. This agrees with the observation that the time of first observable perturbations becomes increasingly smaller as the Reynolds number is increased.

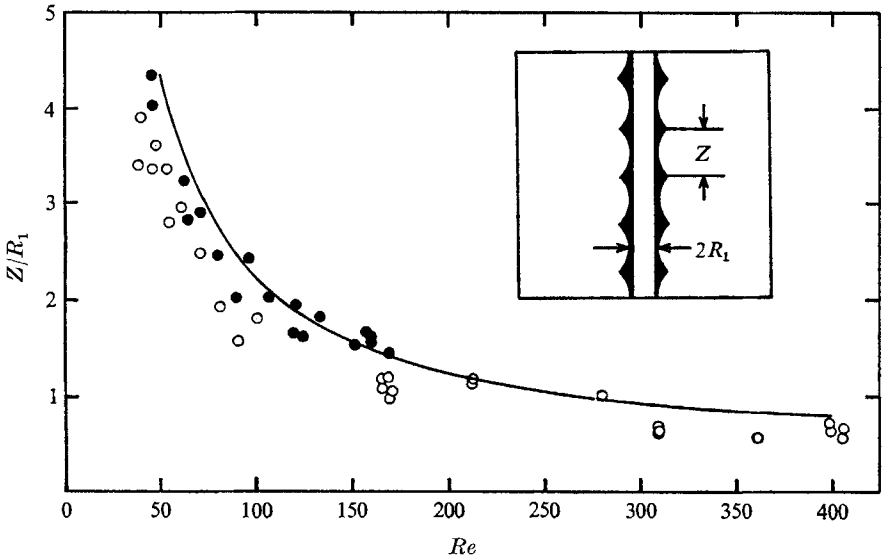

FIGURE 3. Comparison of experimental and theoretical critical wavelength (initial-value problem). ●, data from I, $\eta = 0{\cdot}1$; ○, data from Liu (1971), $\eta = 0{\cdot}2$.

At the minimum point, the perturbation kinetic energy has zero growth. If the basic flow field has not been materially altered due to the cumulative effects of the perturbations, then a quasi-steady analysis at this particular instant should indicate that the basic flow velocity profile is neutrally stable or on the verge of instability. Such calculations are carried out in the following section. Shen (1961) has advanced the idea of momentary stability in which the ratio of kinetic energy of the perturbations to that of the basic flow is examined to determine whether the flow is stable. From the results presented in figure 4, it is seen that the time when the relative kinetic energy $E_r = E_p/E_b$ reaches a minimum is larger than the time for the perturbation kinetic energy to reach a minimum due to continued growth of E_b. The critical times to reach the minimum perturbation kinetic energy E_m, the minimum relative kinetic energy E_{rm}, and a 10^n-fold increase of the perturbation kinetic energy E_n are listed in table 1 for $n = 1$, 2, and 3. These are presented graphically in figure 5 together with the data from I and from Liu (1971). Generally speaking, when the perturbation kinetic energy has increased a thousand-fold the secondary flow pattern has become clearly observable. The critical time of intrinsic instability τ_i which

separates the time zones of decay and growth of the perturbations is about $\frac{1}{4}$ of the time of observable secondary flows. The computation time required on an IBM 360/67 is approximately 1 min for the $Re = 400$ and about 8·5 min for the $Re = 50$ case.

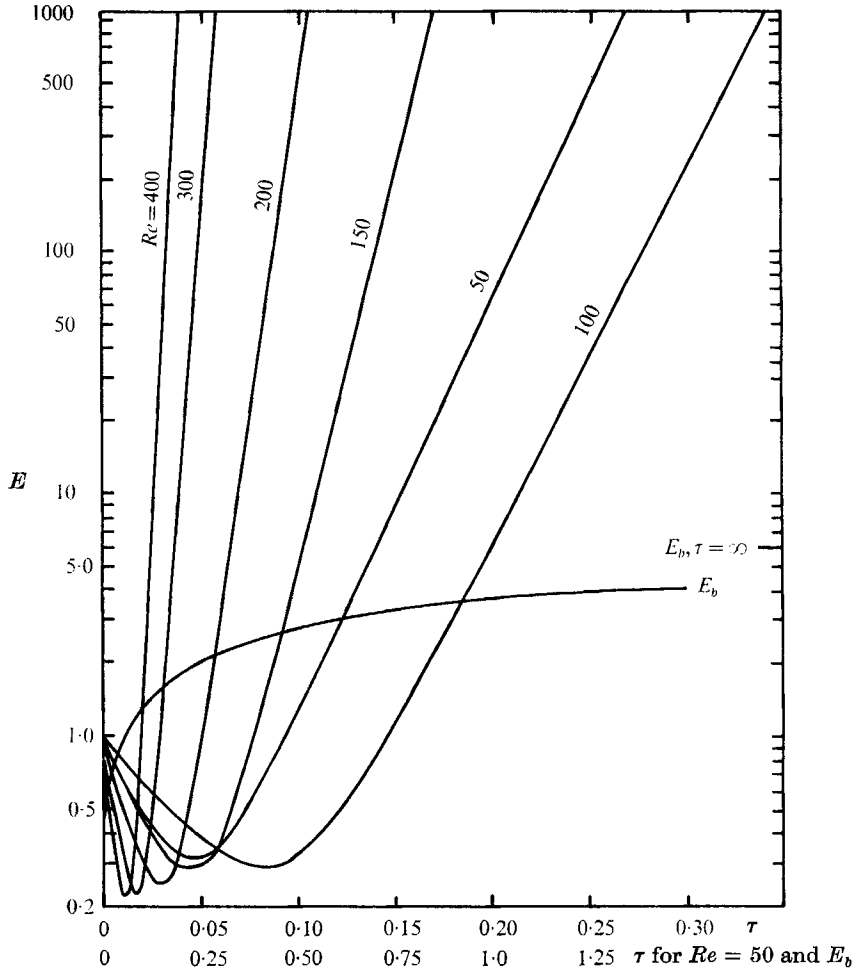

FIGURE 4. Growth curves for the perturbation kinetic energy at the critical wave-number.

It is to be noted that the initial kinetic energy of the perturbations is of the order 10^{-10} to 10^{-8}. After attaining a thousand-fold increase, the perturbation kinetic energy is of order 10^{-7} to 10^{-5} and the perturbation velocity components are of order 10^{-3} to 10^{-2}. The corresponding quantities for the basic flow are of order 1 at the same time. It is seen that linearized theory is still applicable.

Thompson (1968) developed this method to treat the problem of an impulsively started cylinder in a large container. For his numerical computation, he chose an annular region $1 \leqslant r \leqslant 4$. At the outer boundary, the free slip condition is applied. A total of 36 grid points were used, which would correspond to $J = 48$

in the present case. Waves of selected wavelengths were calculated for $Re = 50$, 100 and 150. His results show that the wave which starts to grow first may not attain the fastest growth rate later. No systematic search was carried out to determine the wavelength of the fastest growing wave. In view of our results, the grid size used by Thompson may have been too large for accurate prediction of the growth of the perturbation kinetic energy.

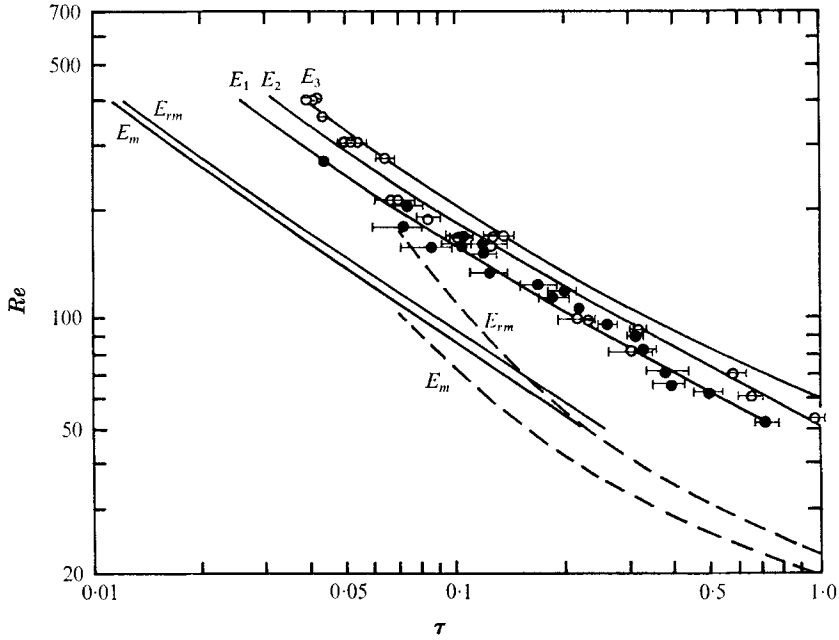

FIGURE 5. Comparison of experimental and theoretical critical times. ●, data from I, $\eta = 0{\cdot}1$; ○, data from Liu (1971), $\eta = 0{\cdot}2$; ——, initial-value problem, $\eta = 0{\cdot}2$; – – –, quasi-steady analysis, $\eta = 0{\cdot}1$, (E_m denotes zero growth rate, E_{rm} denotes momentary stability).

For a radius ratio of 0·2, the critical Reynolds number at which Taylor instabilities occur when the basic flow is steady is 22·1 at a critical wave-number of 0·815 (Walowit, Tsao & DiPrima 1964). The evolution of the perturbation kinetic energy at the critical state is shown in figure 6. It is seen that the initial decay takes place over a long period of time and finally at $\tau = 1{\cdot}25$, it has reached the minimum and begins to grow. In the case of a subcritical Reynolds number 20, the perturbations decay steadily.

From these results a clear picture of the flow has emerged. For impulsively started circular Couette flow with stationary outer cylinder, if the Reynolds number is subcritical ($< 22{\cdot}1$ for $Re = 5$), any perturbation present at the start of the experiment decays steadily. When this Reynolds number is increased beyond the critical, there exists a critical time τ_i, prior to which the initial perturbation decays and beyond which the perturbation grows steadily. It takes time for these perturbations to grow to observable secondary-flow patterns. The

lower the supercritical Reynolds number, the longer it takes for the perturbations to grow into observable secondary-flow patterns.

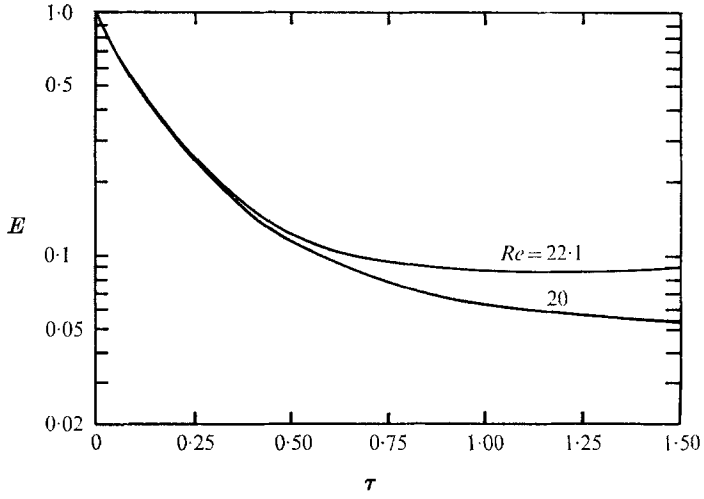

FIGURE 6. Perturbation kinetic energy at critical and subcritical Reynolds numbers, $\kappa = 0{\cdot}815$.

3. Quasi-steady analysis

3.1. *Method of solution*

For a quasi-steady analysis of the problem, we shall examine the instantaneous velocity profile to see whether the disturbances would grow or decay. The velocity components u' and v' are assumed to be

$$u'(r',t) = \bar{u}(r')\,e^{kt}, \quad v'(r',t) = \bar{v}(r')\,e^{kt}. \tag{18}$$

For later application of the Galerkin method, we transform the radial co-ordinate r' into a non-dimensional co-ordinate x where

$$x = \frac{r'}{R_2 - R_1} - \frac{1}{2}\frac{R_2 + R_1}{R_2 - R_1}, \tag{19}$$

so that the boundary surfaces are at $x = \pm\frac{1}{2}$. Substituting (18) and (19) into the basic equation (1) and (2) we obtain the non-dimensional equations

$$[DD^* - a^2 - \sigma][DD^* - a^2]\,u = Ta^2 V v (R_2 + R_1)/2r'(x), \tag{20}$$

$$[DD^* - a^2 - \sigma]\,v = uD^*V, \tag{21}$$

in which the operators D and D^* now stand for

$$D = d/dx \quad \text{and} \quad D^* = d/dx + (R_2 - R_1)/r'(x),$$

and the other non-dimensional symbols are defined as

$$a = (R_2 - R_1)\,\alpha, \quad \sigma = (R_2 - R_1)^2\,k/\nu,$$

$$T = \text{Taylor number} = \frac{4(R_2 - R_1)^4\,V_0'^2}{(R_2^2 - R_1^2)\,\nu^2} = 4R_e^2\eta^2(1-\eta)^3/(1+\eta).$$

All velocites u, v and V have been scaled by the V_0'. In addition, u has been scaled by the dimensionless factor $\nu/V_0'(R_2-R_1)$.

The time-dependent basic flow velocity distribution may be obtained by applying Hankel transforms to (7) together with initial and boundary conditions (8*a*) and (8*b*) as done by Tranter (1956). The solution written in terms of x is

$$V(x,\tau) = \frac{\eta}{\xi}\left(\frac{\xi^2-1}{\eta^2-1}\right) + \sum_{i=1}^{\infty} Q(\lambda_i,\eta)\left[J_1\left(\lambda_i\frac{\xi}{\eta}\right)Y_1(\lambda_i) - J_1(\lambda_i)Y_1\left(\lambda_i\frac{\xi}{\eta}\right)\right]e^{-\lambda_i^2\tau}, \quad (22)$$

where J_1 and Y_1 are Bessel functions,

$$\left.\begin{aligned} Q(\lambda_i,\eta) &= \pi\{[J_1(\lambda_i)/J_1(\lambda_i/\eta)]^2-1\}^{-1},\\ \xi/\eta &= (1+\eta)/2\eta + (1-\eta)\,x/\eta. \end{aligned}\right\} \quad (23)$$

The λ_i's are the roots of the equation

$$J_1(\lambda/\eta)\,Y_1(\lambda) - J_1(\lambda)\,Y_1(\lambda/\eta) = 0. \quad (24)$$

Weil, Murty & Rao (1967) have given the first ten roots of the above equation for $\eta = 0{\cdot}1$. From I, it is known that the flow became unstable at $\tau = 0{\cdot}1$ or less at higher Reynolds numbers. In order to be sure that the basic velocity distribution is correctly evaluated, we have calculated the first fifty roots of (24), and these are listed in table 2.

n	λ_n	n	λ_n
1	0·39409	26	9·0789
2	0·73306	27	9·4287
3	1·0748	28	9·7777
4	1·4189	29	10·127
5	1·7643	30	10·476
6	2·1107	31	10·824
7	2·4578	32	11·173
8	2·8052	33	11·522
9	3·1530	34	11·871
10	3·5010	35	12·220
11	3·8492	36	12·569
12	4·1975	37	12·918
13	4·5459	38	13·267
14	4·8944	39	13·616
15	5·2430	40	13·965
16	5·5917	41	14·314
17	5·9404	42	14·663
18	6·2891	43	15·012
19	6·6378	44	15·361
20	6·9866	45	15·710
21	7·3355	46	16·059
22	7·6843	47	16·408
23	8·0331	48	16·757
24	8·3820	49	17·106
25	8·7309	50	17·455

TABLE 2. First 50 roots of the equation $J_1(\lambda/\eta)\,Y_1(\lambda) - J_1(\lambda)\,Y_1(\lambda/\eta) = 0$, $\eta = 0{\cdot}10$

The basic velocity distributions have been calculated for $\tau = 0{\cdot}1, 0{\cdot}5, 1, 10, \infty$, and are shown in figure 7. It can be seen that at $\tau = 1$ the momentum due to the rotation of the inner cylinder has only diffused to about half of the gap width.

In solving (20) and (21), two stability criteria are examined: the zero-growth rate criterion and the momentary stability criterion. In both cases, the instantaneous velocity distribution of the basic flow is investigated for stability. In the former case, the instantaneous velocity distribution is frozen and it is

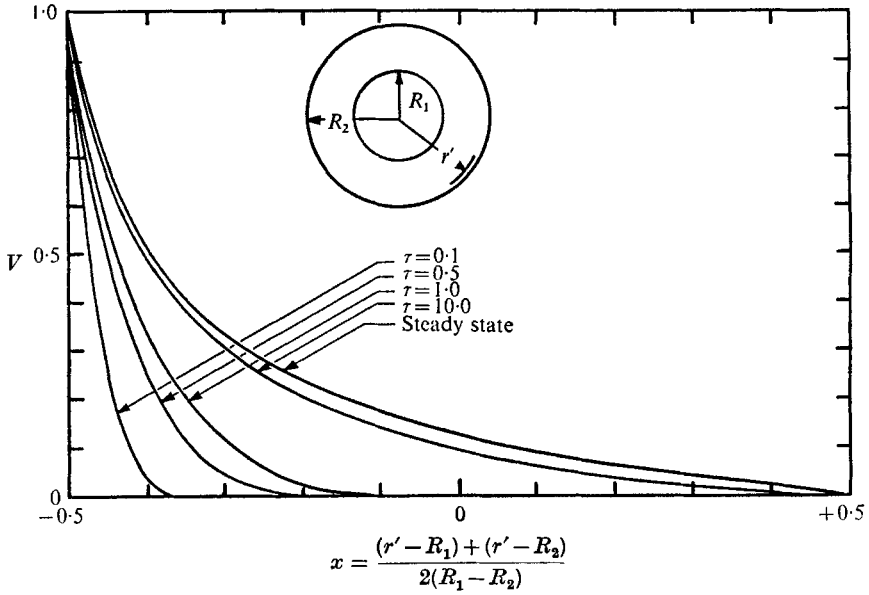

FIGURE 7. Dimensionless velocity distribution as a function of x for various dimensionless times ($\tau = \nu t/R_1^2$). All calculations were made at $\eta = 0{\cdot}1$.

determined whether a superimposed perturbation would grow or decay with increasing time. With this zero growth rate criteria the perturbations are assumed to grow at such a fast rate that the developing basic velocity profile can be considered to be fixed. That is, the time scale for the growth of the perturbations is assumed to be much shorter than the time scale for the developing basic flow profile. The flow is classified as stable or unstable according to the decay or growth of the perturbations. When the principle of exchange of stabilities ($\sigma = 0$) is applied to (20) and (21), we obtain the same eigenvalue problem as that for a steady flow except for the basic velocity profile V. Methods used for investigating the stability of steady flows are equally applicable in this case.

The momentary stability criterion advanced by Shen (1961), on the other hand, examines the growth of the perturbations with respect to the basic flow at any given instant. Thus an accelerated basic flow is unstable only when the perturbations are growing faster, in some appropriate sense, than the basic flow. Thus, a non-zero growth rate of the perturbations ($\sigma > 0$) is tolerated as long as the perturbations are not growing faster than the basic flow. We therefore examine the ratio of the instantaneous kinetic energy of the perturbations to that of the basic flow. The marginal stability condition is determined by the

fact that the growth rate of perturbation kinetic energy is exactly the same as that for the basic flow. With this criterion, the growth rate σ at the marginally stable state is

$$\sigma(\tau) = \frac{1}{2E_B}\frac{dE_B}{d\tau}\left(\frac{1}{\eta}-1\right)^2. \tag{25}$$

The dimensionless growth rate $\sigma(\tau)$ has been evaluated for $\eta = 0{\cdot}1$ and $0 < \tau < 2{\cdot}0$ as shown in figure 8. As expected, $\sigma(\tau)$ becomes very large at small τ due to the strong initial acceleration. When the value of $\sigma(\tau)$ appropriate for a particular time is used in (20) and (21), we obtain an eigenvalue problem slightly modified from the quasi-steady case.

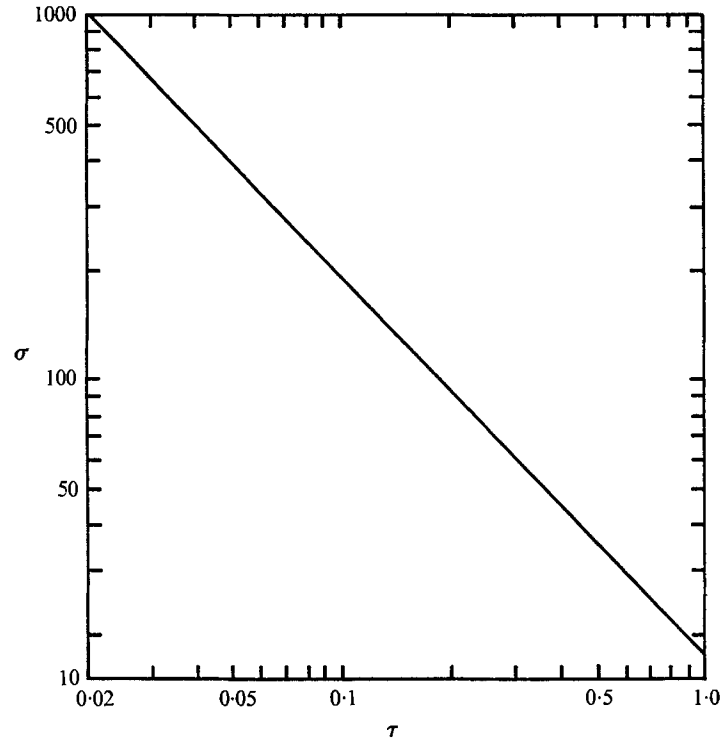

FIGURE 8. Growth rate σ as function of time.

The eigenvalue problem defined by (20) and (21) can be conveniently solved by means of the Galerkin method. This method has been successfully used by Walowit, Tsao & DiPrima (1964) and Tsao (1964) for the steady wide-gap Couette flow problem and by Meister (1963) and Meister & Münzner (1966) on time-dependent narrow-gap Couette flows. According to their experience, the convergence is quite rapid. The eigenfunctions u and v are expanded in complete sets of functions which satisfy the boundary conditions $u = v = Du = 0$ at $x = \pm\frac{1}{2}$. The coefficients in the expansion series are determined by the requirement that the errors in (20) and (21) be orthogonal to the expansion functions u and v. This requirement reduces the equations to an infinite system of linear

homogeneous algebraic equations for the coefficients in the series. In order to have a non-trivial solution, it is necessary that the determinant of the system be zero. This requirement gives a determinantal equation for $T(a, \sigma, \eta)$.

Let $u(x)$ and $v(x)$ be expanded into the following series,

$$u(x) = \sum_{n=1}^{\infty} \alpha_n u_n(x) \quad \text{and} \quad v(x) = \sum_{n=1}^{\infty} \beta_n v_n(x), \tag{26}$$

where

$$u_n(x) = (x^2 - \tfrac{1}{4})^2 x^{n-1} \quad \text{and} \quad v_n(x) = (x^2 - \tfrac{1}{4}) x^{n-1} \quad (n = 1, 2, \ldots). \tag{27}$$

These complete sets of functions have been used by Kurzweg (1961), Walowit *et al.* (1964) and Tsao (1964), in the solution of several steady-state Taylor problems. The inner product of $f(x)$ and $g(x)$ is defined as

$$\int_{-\frac{1}{2}}^{+\frac{1}{2}} f(x)\, g(x)\, \xi\, dx$$

in which the weight function ξ is given by (23). After substituting the M-term eigenfunction expansions into (20) and (21) and requiring that the errors be orthogonal to the expansion functions we obtain,

$$\sum_{n=1}^{M} \alpha_n \left\{ \int_{-\frac{1}{2}}^{+\frac{1}{2}} \xi u_m (DD^* - a^2 - \sigma)(DD^* - a^2) u_n \, dx - \beta_n a^2 T \times \int_{-\frac{1}{2}}^{+\frac{1}{2}} (R_2 + R_1) \frac{\xi u_m V v_n \, dx}{2r'(x)} \right\} = 0, \tag{28}$$

$$\sum_{n=1}^{M} \alpha_n \left\{ \int_{-\frac{1}{2}}^{+\frac{1}{2}} \xi u_n (D^* V) v_m \, dx - \beta_n \int_{-\frac{1}{2}}^{+\frac{1}{2}} \xi [(DD^* - a^2 - \sigma) v_n] v_m \, dx \right\} = 0 \quad (m = 1, 2, \ldots, M). \tag{29}$$

With this choice of expansion functions all of the integrals can be expressed exactly. However, it is more convenient to express the integrals as linear combinations of the following fundamental integrals:

$$S(m, n) = \int_{-\frac{1}{2}}^{+\frac{1}{2}} x^m (x^2 - \tfrac{1}{4})^n \, dx,$$

$$F(m, n, p, \eta) = \int_{-\frac{1}{2}}^{+\frac{1}{2}} \frac{x^m (x^2 - \frac{1}{4})^n \, dx}{\xi^p},$$

$$BJ(m, n, \delta, \lambda_i, \eta) = \int_{-\frac{1}{2}}^{+\frac{1}{2}} x^m (x^2 - \tfrac{1}{4})^n J_\delta \left(\frac{\lambda_i \xi}{\eta} \right) dx,$$

$$BY(m, n, \delta, \lambda_i, \eta) = \int_{-\frac{1}{2}}^{+\frac{1}{2}} x^m (x^2 - \tfrac{1}{4})^n Y_\delta \left(\frac{\lambda_i \xi}{\eta} \right) dx.$$

Here m and n are zero or positive integers, p is a positive integer, and $\delta = 0$ or 1. The details concerning the evaluation of these integrals can be found in Kirchner (1968).

The determinant for given η, σ, and a is a Mth degree polynomial in T. The smallest positive root over all real positive values of a is the approximate value

of the critical Taylor number. The determinant was evaluated using the method of pivotal condensation, the first zero was found using a systematic searching procedure and was refined using the secant method for determining a root. All of the computations were carried out in double precision arithmetic on an IBM-7040.

Calculations have been made for $M = 2$ to 6 for the quasi-steady case in order to ascertain the nature of the convergence of the Galerkin method. Values of a_m/a_6 and T_m/T_6 are calculated for $\tau = 0{\cdot}10, 0{\cdot}25, 0{\cdot}50, 1{\cdot}00, 10{\cdot}0$ and are listed in table 3. It can be seen that for $\tau \geqslant 0.5$, the 6-term approximation yields good results. However, for $\tau < 0{\cdot}5$, the 6-term results are somewhat higher than the

τ	$\frac{a_2}{a_6}$	$\frac{T_2}{T_6}$	$\frac{a_3}{a_6}$	$\frac{T_3}{T_6}$	$\frac{a_4}{a_6}$	$\frac{T_4}{T_6}$	$\frac{a_5}{a_6}$	$\frac{T_5}{T_6}$
0·100	0·417	63·2	0·544	10·3	0·699	3·14	0·864	1·46
0·250	0·472	19·6	0·596	4·41	0·742	1·89	0·899	1·20
0·500	0·548	7·58	0·685	2·34	0·822	1·34	0·945	1·07
1·00	0·684	3·33	0·807	1·47	0·912	1·10	0·982	1·02

TABLE 3. Critical Taylor number and corresponding values of a ratios for $\eta = 0{\cdot}10$ at various dimensionless times. (The subscripts denote the number of terms taken in the approximating series. All values are normalized using the six-term results)

correct ones. Since the order of the determinant to be evaluated is $2M$, we have stopped at $M = 6$ to avoid excessive computation time. The convergence behaviour of the momentary stability case is assumed to be the same as the quasi-steady case. It should be pointed out that the convergence property of the Galerkin method is quite satisfactory when it is applied to time-dependent, narrow-gap Couette flows (Meister 1963), and to steady-state, wide-gap Couette flows (Walowit *et al.* 1964). It is only in the present time-dependent as well as wide-gap case, it fails to yield rapid convergence. In order to achieve greater accuracy, more terms have to be retained in the Galerkin series with concomitant increase in computer time. It may well be that a direct integration scheme such as used by Sparrow, Munro & Jonsson (1964) would have been a more suitable method for the solutions of (20) and (21).

3.2. *Results and discussion*

The values of critical Taylor number and the critical wave-number a for both the zero growth rate and the momentary stability criteria using the 6-term expansion for $0{\cdot}07 \leqslant \tau \leqslant 1{\cdot}0$ and $\eta = 0{\cdot}1$ have been calculated. The Taylor number is converted into the Reynolds number by $Re = 0{\cdot}061419(T)^{\frac{1}{2}}$ and the wave-number converted into the wavelength by $Z/R_1 = 18\pi/a$, and these are tabulated in table 4. The steady-state critical Reynolds number and the wavelength are also listed for reference. The critical wavelengths predicted using either of these two criteria are about the same, and they are about twice the values observed or calculated by the initial-value problem approach. Using the quasi-steady method, we obtain the waves which tend to grow first. On the other hand, with the

initial-value problem approach, we are able to identify that wave which has achieved the fastest growth rate over the entire time period considered. The critical wavelengths obtained by these two methods are not strictly comparable in view of the results obtained by Mahler *et al.* (1968). Using the quasi-steady method, they have shown that the wave which starts to grow first is not the one which sustains the fastest growth rate in an overall sense. We have not, however, carried out computations on the quasi-steady method to ascertain the growth rate of the perturbation at later times for the following reasons. Firstly, in view of

	Zero growth rate criterion		Momentary stability criterion	
τ	Re	Z/R_1	Re	Z/R_1
0·07	103·82	5·39	177·25	3·98
0·08	90·64	5·44	147·63	4·07
0·09	80·90	5·44	126·91	4·16
0·10	73·41	5·49	111·75	4·25
0·15	52·48	5·77	72·51	4·56
0·20	42·78	6·08	56·16	4·88
0·25	37·17	6·35	47·26	5·14
0·30	33·47	6·65	41·66	5·34
0·35	30·85	6·90	37·79	5·60
0·40	28·87	7·16	34·96	5·83
0·5	26·05	7·75	31·05	6·21
0·6	24·11	8·20	28·43	6·65
0·7	22·67	8·70	26·54	7·07
0·8	21·55	9·12	25·09	7·44
0·9	20·64	9·59	23·93	7·85
1·0	19·90	9·92	22·96	8·20
Steady flow	15·70	17·13		

TABLE 4. Critical Reynolds number and wavelengths of quasi-steady analysis with both zero growth rate criterion ($\sigma = 0$) and momentary stability criterion ($\sigma \neq 0$) for $\eta = 0{\cdot}1$. The number of terms taken in the expansion series is 6

the poor convergence of the Galerkin method in the present case, any results obtained would be qualitative at best. Secondly, it has been shown by Mahler *et al.* that the quasi-steady approach over-estimates the growth rate by quite a large margin over that predicted by the initial-value problem approach. This is due to the fact that the ever evolving density profile (or basic velocity profile in our case) is not accounted for using the quasi-steady approach. Although they disclaim any generality of their results, it is our feeling that the same inadequacy of the quasi-steady theory would prevail in the present case.

The critical times for intrinsic instability using either the zero growth rate or the momentary stability criterion are shown in figure 5 with dashed lines and marked E_m and E_{rm}, respectively. It should be remarked here that at the lower values of τ, the correct answers would be to the left of these curves in view of the convergence results shown in table 3. These are comparable to those found in the initial-value problem, confirming once again the results of Mahler *et al.* (1968). However, it is doubtful that the same agreement can be obtained for any earlier

critical time at higher Reynolds numbers. The growth rate σ of the basic flow rises precipitously for $\tau < 0{\cdot}07$ (figure 8) and the concept of quasi-steadiness may no longer be valid.

4. Conclusions

In this paper we have examined the stability of time-dependent Couette flow by two different methods. One is the initial-value problem approach in which the time evolution of the initially present small random perturbations is monitored. With this method we examine the final state of the flow which has evolved in time in order to determine whether the flow is stable. The other is the quasi-steady approach in which the stability of the instantaneous basic velocity profile is analyzed. In this latter method, both the zero growth rate and the momentary stability criteria are examined. With the quasi-steady approach, we examine the state of motion at a particular instant to determine whether the flow is stable with respect to small disturbances.

The results of the initial-value problem show that the perturbation kinetic energy first decays, reaches a minimum, then grows exponentially. The critical wavelength of the fastest growing wave obtained with this method agrees closely with experimental observation of I and Liu (1971). It appears that when the perturbation kinetic energy has grown a thousand-fold, the instability disks are clearly observable. The time of intrinsic instability (the time at which perturbation first tends to grow) is about $\frac{1}{4}$ of the time required for the instability disks to become observable.

The results obtained using the quasi-steady analysis show that the wavelengths of the perturbations which tend to grow first are about twice as large as those calculated by the initial-value problem approach and as those observed experimentally. The critical times for intrinsic instability are comparable to the results of the initial-value problem for $\tau_i > 0{\cdot}07$. At any earlier time, the concept of quasi-steadiness may no longer be valid. These results in general are in agreement with those found by Mahler *et al.* (1968) on an equivalent Bénard problem with suddenly applied cooling from above. Both the zero growth rate and the momentary stability criteria gave approximately the same results.

This research has been supported by the National Science Foundation under Grants GK-1269 and GK-2096. R. P. Kirchner gratefully acknowledges financial aid by NASA (Predoctoral Traineeship) and the Ford Foundation.

REFERENCES

CHEN, C. F. & CHRISTENSEN, D. C. 1967 Stability of flow induced by an impulsively started rotating cylinder. *Phys. Fluids*, **10**, 1845.

CONRAD, P. W. & CRIMINALE, W. O. 1965 The stability of time-dependent laminar flow: flow with curved streamlines. *Z. angew. Math. Phys.* **16**, 569.

CURRIE, J. G. 1967 The effect of heating rate on stability of stationary fluids. *J. Fluid Mech.* **29**, 337.

DONNELLY, R. J. 1964 Experiments on the stability of viscous flow between rotating cylinders, III, enhancement of stability by modulation. *Proc. Roy. Soc.* A **281**, 130.

DONNELLY, R. J. & SIMON, N. J. 1960 An empirical torque relation for supercritical flow between rotating cylinders. *J. Fluid Mech.* **7**, 401.

FOSTER, T. D. 1965 Stability of homogeneous fluid cooled uniformly from above. *Phys. Fluids*, **8**, 1249.

FOSTER, T. D. 1969 Onset of manifest convection in a layer of fluid with a time-dependent surface temperature. *Phys. Fluids*, **12**, 2482.

KIRCHNER, R. P. 1968 The stability of viscous time-dependent flow between concentric rotating cylinders with a wide gap. Ph.D. Thesis, Dept. of Mech. & Aero. Engineering, Rutgers University, New Brunswick, N.J. (Also issued as TR121-MAE-F.)

KIRCHNER, R. P. & CHEN, C. F. 1970 Stability of time-dependent rotational Couette flow. Part 1. Experimental investigation. *J. Fluid Mech.* **40**, 39.

KURZWEG, U. H. 1961 Magnetohydrodynamic stability of curved viscous flows. *Princeton University, Dept. of Physics, Technical Report* II-29.

LICK, W. 1965 The stability of a fluid layer with time-dependent heating. *J. Fluid Mech.* **21**, 565.

LIU, D. C. 1971 Physical and numerical experiments on time-dependent rotational Couette flow. Ph.D. Thesis, Rutgers University (TR-136-MAE-F).

MAHLER, E. G., SCHECHTER, R. S. & WISSLER, E. H. 1968 Stability of a fluid layer with time-dependent density gradients. *Phys. Fluids*, **11**, 1901.

MEISTER, B. 1963 Die Anfangswertaufgabe für die Störungs-differential-gleichungen des Taylorschen Stabilitätsproblems. *Arch. Rat. Mech. Anal.* **14**, 81.

MEISTER, B. & MÜNZNER, W. 1966 Das Taylorsche Stabilitätsproblem mit Modulation. *Z. angew. Math. Phys.* **17**, 537.

MORTON, B. R. 1957 On the equilibrium of a stratified layer of fluid. *Quart. J. Mech. Appl. Math.* **10**, 433.

RICHTMEYER, R. D. & MORTON, K. W. 1967 *Differencing Methods for Initial Value Problems*, 2nd edn. Interscience.

SERRIN, J. 1959 On the stability of viscous fluid motions. *Arch. Rat. Mech. Anal.* **3**, 1.

SHEN, S. F. 1961 Some considerations on the laminar stability of time-dependent basic flows. *J. Aero. Sci.* **28**, 397.

SPARROW, E. M., MUNRO, W. D. & JONSSON, V. K. 1964 Instability of the flow between rotating cylinders: the wide-gap problem. *J. Fluid Mech.* **20**, 35.

TODD, J. 1962 *Survey of Numerical Analysis.* McGraw-Hill.

THOMPSON, R. 1968 Instabilities of some time-dependent flows. Ph.D. thesis, Dept. of Meteorology, Mass. Inst. of Tech.

TRANTER, C. J. 1956 *Integral Transforms in Mathematical Physics.* John Wiley.

TSAO, S. 1964 Stability of flow between arbitrarily spaced concentric cylindrical surfaces and related mathematical problems. Ph.D. thesis, Rensselaer Polytechnic Inst., Troy, N.Y.

WALOWIT, J., TSAO, S. & DIPRIMA, R. C. 1964 Stability of flow between arbitrarily spaced concentric surfaces including the effect of a radial temperature gradient. *J. Appl. Mech.* **31**, 585.

WEIL, J., MURTY, T. S. & RAO, D. B. 1967 Zeros of $J_n(\lambda)\, Y_n(\lambda\eta) - J_n(\eta\lambda)\, Y_n(\lambda)$. *Mathematics of Computation*, **21**, 722.